THE JOURNAL OF PHYSICAL CHEMISTRY C

Article

Cite This: J. Phys. Chem. C 2018, 122, 24652−24657

pubs.acs.org/JPCC

Effects of Fluid Confinement and Temperature in Supported Acetophenone Films

Samantha L. Nania, Jaclyn Wrona, and Scott K. Shaw*

Department of Chemistry, University of Iowa, W476 Chemistry Building, Iowa City, Iowa 52242, United States.

Supporting Information

ABSTRACT: Solid−liquid phase transitions are thought to be well understood in bulk phases of matter, but in thin films or interfacial volumes, melting and freezing transitions can exhibit significant departures from expected behaviors. Here, we show multiple solid−liquid phase transitions in thin films (50−500 nm) of the molecular fluid acetophenone. Transitions are driven by both geometric confinement and temperature, as characterized by spectroscopy. Fluid film confinement is controlled by systematic variation of the supported film thicknesses, and the same films are passed through cooling−heating cycles to generate amorphous or crystalline films with distinctly different molecular environments. Specifically, multiple temperature cycles reveal a distinct conditioning dependence, wherein phase transitions may or may not exhibit significant changes in the infrared absorption profile over the temperature cycle, indicating distinct crystalline and liquid-like phases. Significant effects of supercooling are also observed as a result of the highly confined nature of the thin-film sampling geometry. Interestingly, the spectral profiles recorded as a function of film temperature show clear evidence of molecular reordering phase transitions, which is similar to observations in variable thickness films held at constant temperature. The changes in spectral absorption profiles confirm the confinement-induced crystalline ordering and provide evidence that molecular confinement effects can extend beyond 100 nm from a surface, which is much larger than conventionally accepted "interfacial" volumes. Ultimately, the extended crystalline ordering within liquid films could offer important new avenues to tune the physical properties of designer interfaces.

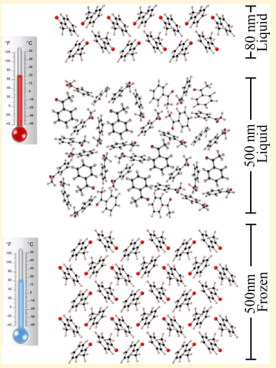

INTRODUCTION

Solid−liquid interfaces play important roles in many everyday applications. Knowledge of the key intermolecular interactions is essential to recognize and improve the roles of chemicals and materials used in these applications. While the interfacial region is typically difficult to study because of its small dimensions, applications of advanced analytical methods have revealed the general trends of molecular ordering near surfaces and revealed the significant departures from the resulting bulk-phase properties.[1−3] Density profiles can be helpful in visualizing the ordering, similar to that shown in Figure 1. The periodic oscillation in the density profile results from the periodic order found in fluid layers near surfaces, which creates an anisotropic interfacial volume. The mass density increases at the center of each layer of molecular packing and then decreases between the layers. These periodic density fluctuations decay with increasing distance from the surface as the fluid increasingly assumes an isotropic, bulk-like, configuration.[4]

Solid-like properties have been reported for thin films confined to the interface in a variety of fluids and experimental geometries.[3,5−11] Solid-like behavior at the interface has been shown, for instance, by Israelachvili et al. when probing liquid to solid transitions of spherical, chain-like, and branching molecules.[3] Regardless of shape, the molecules display a liquid-like behavior when unconfined by the plates of a surface force apparatus (gap size > five molecular layers), but the molecules exhibit a solid-like behavior when they are more confined (gap size < five molecular layers). This indicates that confining a liquid may be a route to creating molecular-scale ordering and tuning critical material properties.[3] Dutta et al. have reduced

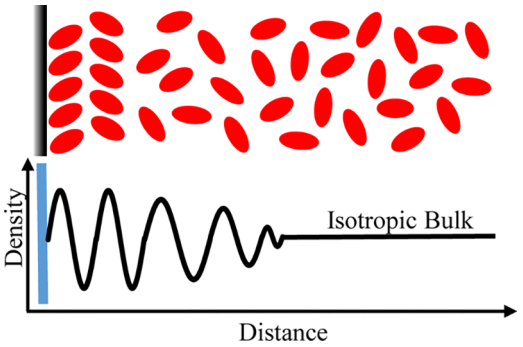

Figure 1. Top: Schematic of molecular ordering as a function of distance from the surface showing the molecules at the interface ordering in layers parallel to the interface, while those farthest away are random and isotropic. Bottom: Density profile representing the ordering at the interface until the fluctuations decay into the bulk. Figure adapted from Granick (ref 4).

Received: April 28, 2018
Revised: May 29, 2018
Published: June 6, 2018

DOI: 10.1021/acs.jpcc.8b04051
J. Phys. Chem. C 2018, 122, 24652−24657

the number of necessary solid, confining surfaces to one, showing that layering occurs near a single surface for tetrakis(2-ethylhexoxy)silane, where the liquid films diverge from the ideal isotropic structure.[2,12,13] Furthermore, Weeks et al. have shown that a simple solvent such as acetonitrile shows ordered layers that extend ca. 2 nm from a single silica surface.[14] Because the orientation and ordering of molecules at a surface can change the properties and dynamics of devices of which they are a part, the ability to quantify and control interfacial molecular architectures is a fruitful research area.

Previously, our group has reported creating and observing chemical interfaces via a dynamic wetting technique.[15] In this technique, a stable liquid film of tunable thickness is created on a vertical solid substrate (Figure 2). By varying the velocity of the substrate, the properties of molecules within the film can be analyzed as a function of film thickness. This study shows that as the films thin, increased confinement can lead to solid-like phases even at temperatures well above the melting point of the fluid in question. Specifically, we found that the infrared (IR) spectra for the thin (80 nm) acetophenone film is comparable to that of a bulk frozen film, indicating that the confinement within the interfacial volume is conducive to crystallization.[15]

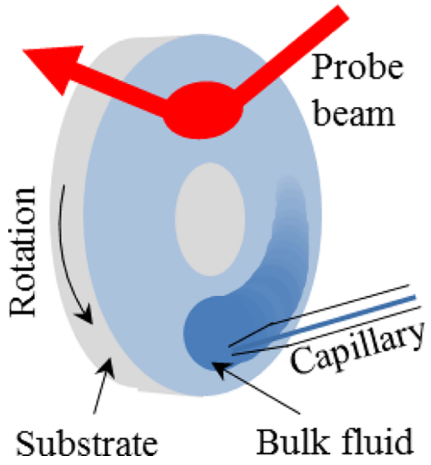

Figure 2. Cartoon schematic of dynamic wetting sampling geometry.

The objective of the present work is to test our ability to control the molecular ordering of acetophenone within thin confined films by applying desired temperature programs. Hence, we utilize thermal analysis coupled to IR spectroscopy to qualitatively identify phase transitions such as crystallization, glass transitions,[16] cold crystallizations,[17] and melting. Identifying these phase changes is critical to controlling the chemical properties and orientations as the temperature is systematically varied.

Using the dynamic wetting technique described above, we create thin fluid films (50−500 nm) and vary the temperature of the surface through consecutive freeze-and-melt cycles. We interpret IR spectral profiles to report the molecular behavior and ordering of acetophenone at the solid−liquid interface as a function of film thickness and temperature.

EXPERIMENTAL SECTION

Surface Preparation. Silver disks with a diameter of 14 mm (polycrystalline, 99.999%, ESPI Metals) are mechanically polished using aluminum oxide abrasive powder and chemically polished using a chromate etch procedure described in previous publications[18,19] to achieve mirror-like polishes, <4 nm root-mean-square roughness (atomic force microscopy). Surface cleanliness is confirmed before measurements using polarization modulation-infrared reflection−adsorption spectroscopy (IRRAS).

Materials. H_2SO_4 (ACS grade, BDH), $HClO_4$ (70%, Sigma), NH_4OH (28−30%, BDH), and acetophenone (98%, Acros Organics) are used as received. Solutions of CrO_3 (99.9%, Aldrich) and HCl (ACS grade, BDH) are prepared at 4.0 and 0.6 M, respectively, with Milli-Q water. Water is purified with a Milli-Q UV Plus System (Millipore Corp) to reach 18.2 MΩ cm resistivity, TOC ≤ 4 ppb.

INSTRUMENTAL METHODS

Temperature-Controlled Dynamic Wetting. A brass shaft is attached to a gear head-variable voltage (0−12 V) dc motor combo (MicroMo) and enclosed in a cylindrical poly(tetrafluoroethylene) (PTFE) plunger. The brass shaft is sealed at either end by ceramic, nonlubricated ball bearings. These ball bearings form a sealed chamber around the brass shaft while allowing free rotation of the shaft, independent of the PTFE plunger (Figure S1). A polished silver disk substrate is mounted on the end of the brass shaft, and the plunger assembly is inserted into the nitrogen-purged PTFE cell body. The cell volume is air-tight, creating a controlled sampling environment. The cell is fitted with two CaF_2 windows (25 mm × 1 mm UV grade, Crystran Limited) for spectroscopic access. Before creating fluid films, a droplet of the desired fluid is dispensed into the bottom of the cell, and the nitrogen purge is stopped. This allows a saturated vapor environment to be formed (as monitored by IR absorbance). To create fluid films, a glass capillary is positioned ca. 1 mm from the face of the silver surface, and a droplet of fluid (ca. 250 μL) is dispensed. The droplet contacts the bottom of the silver substrate and is held between the silver substrate and the tip of the glass capillary by capillary forces. The silver substrate is then rotated through the bulk droplet at a desired velocity, extruding a thin film across the surface.

No fluid is consumed to maintain a film of desired thickness, so once a stable film is created, the capillary is pulled away from the substrate. The temperature of the substrate is regulated by flowing a large volume of gas across the brass shaft (Figure S1). High thermal conductivity of the brass shaft conducts heat to and from the substrate. The heated or cooled gas that contacts the brass shaft is chemically isolated from the substrate itself. Only thermal energy flows through the connecting brass shaft. Variable fluid temperature and flow rate allow control of the silver substrate temperature. The temperature of the sample surface and the surrounding cell vapor/gas phase are measured continuously using calibrated thermocouples (Automation Direct model: Solo 4824).

The substrate continuously rotates as the temperature is varied from room temperature to the point at which the film freezes. Once the film freezes, the rotation of the substrate is stopped to reduce the interference from variable film thicknesses that develop naturally across the vertical face of the substrate. To melt the film, the surface is warmed and rotation is restarted to ensure that the film thickness remains stable. IR spectra are collected continuously throughout the entire temperature cycle. Film thicknesses are determined via spectroscopic ellipsometry as described in the Supporting Information and in more detail in previous publications.[15]

DOI: 10.1021/acs.jpcc.8b04051
J. Phys. Chem. C 2018, 122, 24652−24657

Infrared Reflection−Adsorption Spectroscopy. The IR beam from a Thermo-Nicolet iS50 Fourier transform spectrometer is directed to an external optical table, which is enclosed and purged with dry CO_2-free air. The IR beam is reflected from a collimating mirror and passed through a wire grid polarizer, which selectively transmits p-polarized light. The polarized IR beam enters the dynamic wetting cell through the disk-shaped CaF_2 window. The cell is positioned, so the beam reflects from the surface at an incident angle of 78° ± 3° from surface normal and exits the cell through a second CaF_2 window. The beam is then collected and focused by an additional collimating mirror into a liquid nitrogen-cooled MCT-A detector element. Both the background IRRAS spectrum of bare silver in a nitrogen gas environment and bare silver surface in an acetophenone-saturated vapor environment are taken for reference and background subtractions. The background spectra are averaged over 1000 scans. All IRRAS spectra are collected at a resolution of 4 cm^{-1}. During the cooling cycles, the spectra are averaged over 100 scans. For the heating cycle, the spectra are averaged over 10 scans to increase the time resolution, improving the observation of spectral changes because of small temperature changes.

Temperature-Controlled Transmission Fourier Transform Infrared. Temperature-controlled transmission vibrational spectroscopy measurements are performed using a Thermo-Nicolet iS50 Fourier transform spectrometer with a liquid nitrogen-cooled MCT-A detector. The transmission compartment is equipped with a CryoTherm accessory (International Crystal Laboratories) that enables temperature control within the range of −180 to 250 °C. The accessory includes a vacuum jacket, sealed using KBr windows, along with a liquid nitrogen-cooled refrigerant chamber that encases the cell. The variable temperature cell contains two 4 mm thick CaF_2 windows. The background spectra of clean windows are taken at each temperature of interest. Fluid is dispensed between the windows, and the spectra are collected at the same temperatures as the referenced background spectrum. All transmission spectra are averaged over 32 scans with a resolution of 4 cm^{-1}.

RESULTS AND DISCUSSION

As the thick (500 nm) film of acetophenone thins to ca. 100 nm at room temperature, the molecules exhibit a solid-like crystalline ordering.[15] Figure 3 shows a series of acetophenone wetting spectra at different thicknesses (Table S1), highlighting this change in the absorption features in the 1200 to 1300 cm^{-1} region. These peaks are attributed to bulk and interfacial modes of the C−CO−C bending from the ketone functional group on the molecule. As the film thickness decreases from 1280 ± 392 to 80 ± 6 nm, the molecules in the film become increasingly confined by the parallel surfaces (solid substrate and the overlying vapor phase). This confinement is tracked by the absorption feature at 1250 cm^{-1} shifting to 1262 cm^{-1} (vertical dotted arrow), and the feature at 1274 cm^{-1}, which is attributed to bulk acetophenone, decreases the intensity until, in the thinnest film (80 nm), it disappears. Ultimately, the IR profiles of the thinnest films closely match the IR profile of the frozen acetophenone film (acquired at 17 °C). These results indicate two simultaneous processes: (1) the loss of the bulk material as the film thins and (2) the ordering of the remaining molecules to resemble the architecture of frozen or crystalline acetophenone.

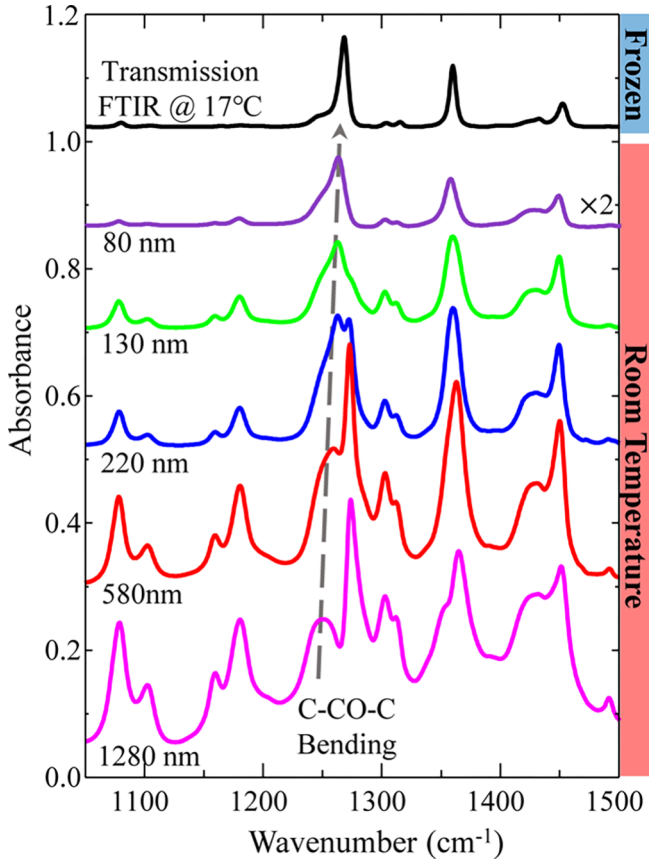

Figure 3. IR spectra of acetophenone. A transmission spectrum of frozen acetophenone (at top) is compared to a series of IRRAS wetting spectra acquired at room temperature for various film thicknesses. The absorption feature at ca. 1265 cm^{-1} is highlighted with an arrow to show the significant wavenumber shift toward the profile of the frozen spectrum as the film thins. The spectra are offset vertically for clarity.

To investigate the combined effects of confinement and temperature, we add temperature control to the stable films of controllable thickness created by the dynamic wetting approach. For these experiments, a silver substrate is rotated at a desired velocity, that is, of 0.076 cm s^{-1}, creating a corresponding film thickness of 500 ± 70 nm. When the film is at room temperature, the film shows an isotropic, bulk liquid-like behavior. During the first cooling cycle, the surface is taken to −5.5 ± 3.9 °C, well below the melting point of 19 °C, before the liquid-to-solid phase transition occurred. This supercooling effect is also seen in bulk acetophenone via differential scanning calorimetry (Figure S2) where the crystallization peak appears at −32.5 ± 2.6 °C. The temperatures at which these changes occur vary greatly from the bulk fluid to thin interfacial films, which we attribute to significantly different chemical environments in thin films. The data in Figure 4 represent changes in the IR profile from cold to hot (top to bottom) observed for the first freezing−melting cycle of the film. The top of Figure 4 (pink-green) shows the first spectrum of the thin interfacial frozen film (at −2.3 °C). A sharp feature at 1272 cm^{-1} is present between −2.3 and 15.1 °C until the film melts (ca. 16.6 °C), at which point the absorption profile returns to that of the liquid-like film, shown in the lower black trace. This absorption profile again exhibits the features from the C−CO−C bending for both the bulk and

DOI: 10.1021/acs.jpcc.8b04051
J. Phys. Chem. C 2018, 122, 24652−24657

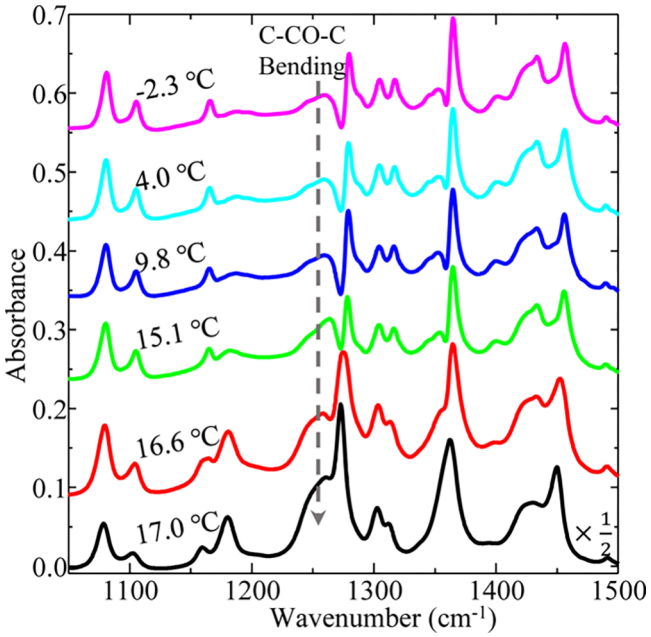

Figure 4. Series of IRRAS spectra acquired during the first warming cycle, from −2.3 to 17 °C (top to bottom). The data show the evolution of several spectral features as the film progresses from frozen (bottom) to melted (top).

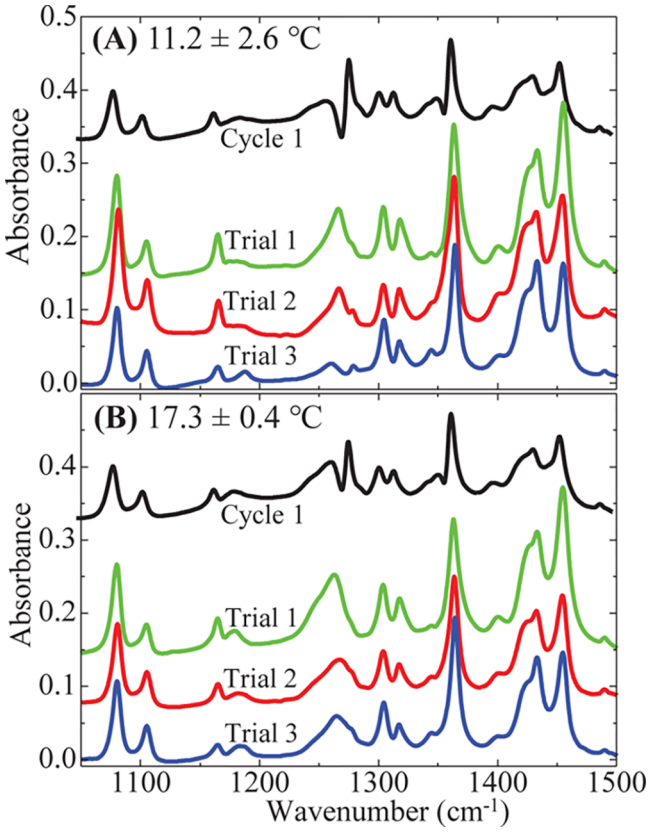

Figure 5. Series of IRRAS spectra collected for (A) immediate frozen/domain ordering and (B) crystalline frozen for the first cycle (black) and for multiple trials of the subsequent cycles to show variation in the spectrum when the film freezes initially. These variations in vibrational profiles suggest that there are different molecular environments or frozen ordered domains at the interface.

interfacial acetophenone at 1274 and 1250 cm^{-1}, respectively. There is also sharpening of the features at around 1350 cm^{-1} (−CH bending due to the methyl) and 1425 cm^{-1} (−CH bending from the ring and methyl). The narrowed line widths are indicative of the film freezing and a better definition between ordered and disordered environments within the films' volume.

After the system has passed through the liquid-to-solid phase transition once, subsequent temperature cycles (cycles 2 thru 4) show vastly different temperature-dependent features. Figure 5 includes spectra at selected temperatures for subsequent cooling−heating cycles. Major differences between the first cycle and subsequent cycles are evident by comparing the top black spectrum to the bottom three trials for subsequent cycles (cycles 2−4). Specifically, the sharp feature at 1272 cm^{-1} seen in the first temperature cycle disappears in subsequent cycles. Multiple trials are shown for subsequent cycles to emphasize variations in spectra immediately after freezing (11.2 ± 2.6 °C) compared to the film that warms (17.3 ± 0.4 °C). In cycles 2−4, the spectra observed immediately after the fluid is frozen, at 11.2 ± 2.6 °C, are seen in Figure 5A. The vibrational profile of the fluid at this point varies only slightly over multiple trials, indicating that an annealing process is completed over the first heating−cooling cycle. The intensity ratios of absorbance peaks between 1200 and 1300 cm^{-1} are highly variable throughout the trials, suggesting that various molecular environments/frozen domains are present as the film is cooled quickly. However, as the frozen/refrozen film warms and approaches the melting point of 19 °C in each cycle, the spectra shift and exhibit similar features across cycles 2 thru 4. The spectra in Figure 5B, acquired at 17.3 ± 0.4 °C, show this change. The emergence of a single peak at around 1268 cm^{-1} is assigned to the interfacial crystalline peak for C−CO−C bending. We predict that the crystallization event in the first thermal cycle may create nucleation sites/domains that endure the thermal cycling (possibly stabilized by proximity to the surface), which serve to seed the film's crystallization in later thermal cycles. The presence of such "surface seeds" is unconfirmed, but their size distributions, orientations, and other properties would make for exciting future work in this area. To better understand the unique spectral features that emerge during the warming process, Figure 6 shows a comparison of a transmission Fourier transform infrared (FTIR) spectrum of frozen acetophenone (17 °C), a liquid room-temperature 80 nm film, and a liquid 500 nm film, after it has been frozen and then warmed to 17.3 ± 0.4 °C, which is just below the reported melting temperature for acetophenone, both acquired by IRRAS. The profile of the feature at 1268 cm^{-1} of the frozen 500 nm film, at 17.3 ± 0.4 °C, matches both the thin 80 nm film and the frozen transmission infrared spectra of acetophenone, suggesting that warming the frozen film allows the acetophenone molecules to undergo a cold-crystallization phase transition.[17] The vibrational spectroscopy of the post-cold crystallization closely resembles that previously observed in thinned (80 nm) films, representing a confined molecular environment (purple trace in Figure 6) even though the film in this case is significantly thicker.[15] The bottom two spectra in Figure 6 show the 500 nm film below melting and above melting temperatures. The growth of the peak at 1274 cm^{-1} and the shifting of the peak from 1268 to 1247 cm^{-1} as the thick film warms are diagnostic of the vastly different

DOI: 10.1021/acs.jpcc.8b04051
J. Phys. Chem. C 2018, 122, 24652−24657

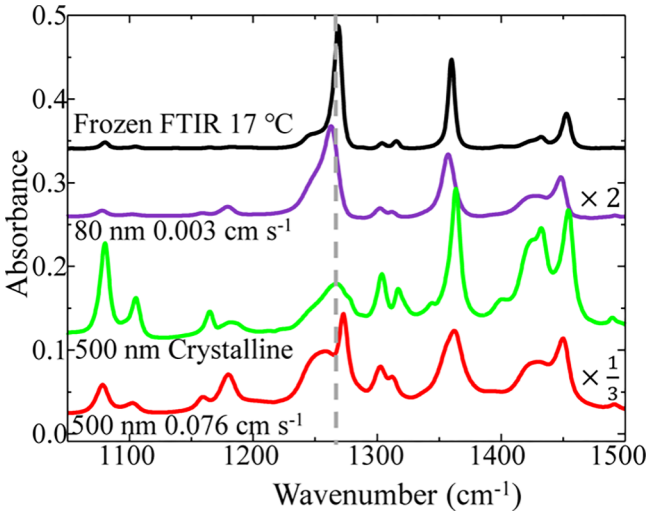

Figure 6. Comparison of the temperature-controlled frozen transmission infrared spectrum at 17 °C (black), the IRRAS wetting spectrum of the thinnest film (80 nm @ rotational velocity of 0.003 cm s^{-1}) (purple), temperature-controlled crystalline frozen spectrum of 500 nm film (green), and the IRRAS wetting spectra of the same 500 nm film at room temperature (decreased by a factor of 1/3 for scaling) (red). A dotted line has been placed to show resemblance between frozen FTIR, wetting 80 nm film, and crystalline 500 nm film.

environments present in crystalline ordering and liquid-like isotropic bulk.

A series of spectra outlining the vibrational changes, which take place during the heating sweep of a postconditioning temperature cycle, are outlined in Figure 7. Starting at the top of the figure, a spectrum of acetophenone is observed at a stable fluid film thickness of 500 nm at room temperature (red dashed). The second spectrum in the series (cyan) is taken immediately after the liquid-to-solid phase transition at 11.2 ± 2.6 °C, followed by the sequential spectra collected during the heating cycle until the film melts at 18.5 ± 0.2 °C (solid red). The spectral similarities between the initial liquid spectrum and the final melted spectrum confirm that the film thickness does not change significantly from start to finish of the temperature cycle, ensuring that the changes seen are not related to any change in the thickness of the films. The vertical dashed line is added to highlight the same peaks of interest from the thickness-dependent data at room temperature seen in Figure 3. The features seen between 1230 and 1300 cm^{-1} in Figures 7 and 3 are strikingly similar (side-by-side in Figure S3) but are performed under very different conditions: varying temperature and varying thinning and confinement, respectively. In both cases, there is a peak at 1262 cm^{-1} that shifts to 1250 cm^{-1} as the film both warms and becomes thicker, while the peak at 1274 cm^{-1} is observed as a function of warming and increased thickness. Because these peaks relate to the molecular environments and degree of interfacial ordering, we conclude that the changes seen for the temperature program are the same type of ordering process that occurs under increasing confinement (thinner films). This reveals important chemical insights into developing crystalline ordering at the interface as a function of both temperature (phase transition) and film thickness (surface confinement).

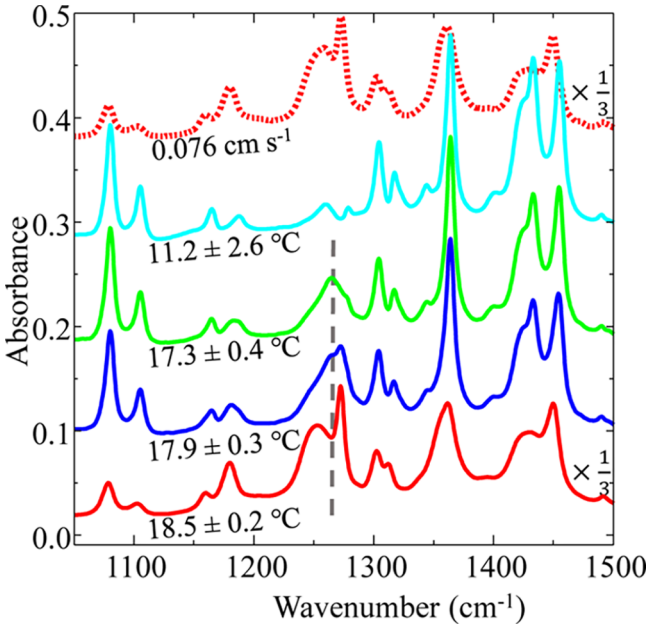

Figure 7. From top to bottom: IRRAS spectra collected at temperature points of the 500 ± 70 nm thick acetophenone film post conditioning through the cooling and heating cycle. The top and bottom spectra have been decreased by a factor of 1/3 for scaling. The absorption feature at ca. 1265 cm^{-1} is highlighted with an arrow to demonstrate that the same features are seen in the warming film as in the thinning films.

CONCLUSIONS

As molecules become confined to an interface, significant changes in their ordering behavior resemble that seen in a bulk frozen fluid. To further understand the crystalline-like nature of molecules as they become geometrically confined, temperature-controlled studies of molecular fluid films were performed as films were taken through multiple cycles of liquid-to-solid phase transitions. During the first temperature cycle in a 500 nm film, the fluid was supercooled to 25 °C beyond the melting point in order to observe the liquid-to-solid phase transition. This first temperature cycle resulted in a sharp feature at 1272 cm^{-1}, which persists over the range of temperatures until the film melts. This feature is not present in subsequent cooling and heating cycles, indicating that a conditioning, or annealing, process is necessary before more characteristic changes in molecular ordering are observed throughout phase transitions. This could be important when considering applications such as lubrication, in which materials pass through multiple temperature cycles.

In the subsequent temperature cycles (cycles 2−4), significant changes were seen in the vibrational profile throughout the temperature cycle relating to the ordering of the molecules. Immediately after the liquid-to-solid phase transition occurred, the resulting spectra showed variations in the IR absorption profiles over each trial conducted here. This suggests a corresponding array of molecular environments upon freezing and indicates numerous domains of ordering upon freezing. The variance in vibrational profile disappears as the film warms and approaches the melting point (19 °C) but is still in the solid state. At 17.3 ± 0.4 °C, the feature at 1268 cm^{-1} emerges, which represents the interfacial crystalline peak for C−CO−C bending. This feature closely resembles what is seen in the room-temperature 80 nm IRRAS film and the frozen transmission FTIR of acetophenone. These similarities

DOI: 10.1021/acs.jpcc.8b04051
J. Phys. Chem. C 2018, 122, 24652−24657

in the vibrational profile as a function of temperature and thickness confirm crystalline ordering in thin films, providing evidence that these confinement effects can extend to significant distances (100 nm) from a wall or other surfaces when exposed to lower temperatures.

By comparing the series of spectra seen in the heating cycle of a 500 nm film, as it progresses from solid to liquid, and the series of spectra seen as the film thickens from 80 to 580 nm, we see that the sequential changes in the two series are strikingly similar for the peaks present in the 1200 −1300 cm^{-1} range. Our results indicate that the ordering process a film undergoes when confined to bulk at constant temperature is similar to that of the ordering induced by thermal processes. These results suggest that surface-induced ordering transitions can be controlled in multiple ways and that the affected volumes of liquids can be much larger than previously thought. Continued experiments in this area will be instrumental in understanding how ordering affects the properties of fluids at the solid−liquid interface.

■ ASSOCIATED CONTENT

Supporting Information

The Supporting Information is available free of charge on the ACS Publications website at DOI: 10.1021/acs.jpcc.8b04051.

Schematic of the dynamic wetting apparatus, table of experimental film thickness of acetophenone with respect to the substrate rotational velocity, differential scanning calorimetry thermogram of bulk acetophenone, and IRRAS spectra seen in Figures 7 and 3 side-by-side for ease of spectral comparisons of features seen between 1230 and 1300 cm^{-1} (PDF)

■ AUTHOR INFORMATION

Corresponding Author

*E-mail: scott-k-shaw@uiowa.edu (S.K.S.).

ORCID

Scott K. Shaw: 0000-0003-3767-3236

Notes

The authors declare no competing financial interest.

■ ACKNOWLEDGMENTS

The authors gratefully acknowledge the funding support from the University of Iowa, the Research Corporation for Science Advancement via a Cottrell Scholar award, and the National Science Foundation under award CHE-1651381.

■ REFERENCES

(1) Butt, H.-J.; Graf, K.; Kappl, M. *Physics and Chemistry of Interfaces*; Wiley-VCH: Germany, 2013.

(2) Yu, C.-J.; Richter, A. G.; Datta, A.; Durbin, M. K.; Dutta, P. Observation of Molecular Layering in Thin Liquid Films Using X-Ray Reflectivity. *Phys. Rev. Lett.* **1999**, *82*, 2326−2329.

(3) Gee, M. L.; McGuiggan, P. M.; Israelachvili, J. N.; Homola, A. M. Liquid to Solidlike Transitions of Molecularly Thin Films Under Shear. *J. Phys. Chem.* **1990**, *93*, 1895−1906.

(4) Granick, S. Motions and Relaxations of Confined Liquids. *Science* **1991**, *253*, 1374−1379.

(5) Israelachvili, J. N.; McGuiggan, P. M.; Homola, A. M. Dynamic Properties of Molecularly Thin Liquid Films. *Science* **1988**, *240*, 189.

(6) Van Alsten, J.; Granick, S. Molecular Tribometry of Ultrathin Liquid Films. *Phys. Rev. Lett.* **1988**, *61*, 2570−2573.

(7) Van Alsten, J.; Granick, S. The Origin of Static Friction in Ultrathin Liquid Films. *Langmuir* **1990**, *6*, 876−880.

(8) Van Alsten, J.; Granick, S. Shear Rheology in a Confined Geometry: Polysiloxane Melts. *Macromolecules* **1990**, *23*, 4856−4862.

(9) Van Alsten, J.; Granick, S. Tribology Studied Using Atomically Smooth Surfaces. *Tribol. Trans.* **1990**, *33*, 436−446.

(10) Homola, A. M.; Israelachvili, J. N.; Gee, M. L.; McGuiggan, P. M. Measurements of and Relation Between the Adhesion and Friction of Two Surfaces Separated by Molecularly Thin Liquid Films. *J. Tribol.* **1989**, *111*, 675−682.

(11) Homola, A. M.; Nguyen, H. V.; Hadziioannou, G. Influence of monomer architecture on the shear properties of molecularly thin polymer melts. *J. Phys. Chem.* **1991**, *94*, 2346−2351.

(12) Yu, C.; Evmenenko, G.; Kmetko, J.; Dutta, P. Effects of Shear Flow on Interfacial Ordering in Liquids: X-ray Scattering Studies. *Langmuir* **2003**, *19*, 9558−9561.

(13) Lee, D. R.; Dutta, P.; Yu, C.-J. Observation of a Liquid-to-Layered Transition in Thin Liquid Films when Surface and Interface Regions Overlap. *Phys. Rev. E: Stat., Nonlinear, Soft Matter Phys.* **2008**, *77*, 030601.

(14) Berne, B. J.; Fourkas, J. T.; Walker, R. A.; Weeks, J. D. Nitriles at Silica Interfaces Resemble Supported Lipid Bilayers. *Acc. Chem. Res.* **2016**, *49*, 1605−1613.

(15) Nania, S. L.; Shaw, S. K. Structural Changes in Acetophenone Fluid Films as a Function of Nanoscale Thickness. *Langmuir* **2017**, *33*, 1623−1628.

(16) Robinson, J.; Skelly Frame, E. G. F. *Undergraduate Instrumental Analysis*, 6th ed; Marcel Dekker: New Youk, 2005.

(17) Faria, L. F. O.; Matos, J. R.; Ribeiro, M. C. C. Thermal Analysis and Raman Spectra of Different Phases of the Ionic Liquid Butyltrimethylammonium Bis(trifluoromethylsulfonyl)imide. *J. Phys. Chem. B* **2012**, *116*, 9238−9245.

(18) Smoliński, S.; Zelenay, P.; Sobkowski, J. Effect of Surface Order on Adsorption of Sulfate Ions on Silver Electrodes. *J. Electroanal. Chem.* **1998**, *442*, 41−47.

(19) Kibler, L. A. *Preparation and Characterization of Noble Metal Single Crystal Electrode Surfaces*; International Society of Electrochemistry: Barcelona, 2003.